applied sciences

MDPI

Article

SATCOM Earth Station Arrays Anti-Jamming Based on MVDR Algorithm

Yanpeng Xi *, Jian Liu and Wenhao Zhao

School of Information and Navigation, Air Force Engineering University, Xi'an 710077, China; sdwfliuj@163.com (J.L.); xs17744962274@126.com (W.Z.)
* Correspondence: xiyanpeng0522@126.com

Abstract: In modern life, a large amount of information is transmitted through satellites. The anti-jamming ability of satellite communication earth stations is the basis for ensuring the smooth flow of information. In the case that multiple small earth stations cannot communicate due to jamming, the minimum variance distortionless response (MVDR) algorithm based on reflector antenna array is proposed. Firstly, the gain expression of satellite communication earth station antenna is derived, and the mathematical model of the received signal of the reflector antenna array is established. Then, the MVDR beamforming algorithm based on the reflector antenna is proposed and applied to the satellite communication earth station reflector antenna array, and the anti-jamming capability of the reflector antenna array using this algorithm is analyzed through simulation. The simulation results show that the earth station reflector antenna array using MVDR algorithm can effectively achieve array gain of the direction of the satellite signal, suppress the jamming signals, increase the output signal to interference plus noise ratio (SINR) of the reflector antenna array, and increase the output signal to jamming plus noise ratio with the increase in the number of snapshots.

Keywords: satellite communication; jamming suppression; antenna array; minimum variance distortionless response (MVDR)

check for updates

Citation: Xi, Y.; Liu, J.; Zhao, W. SATCOM Earth Station Arrays Anti-Jamming Based on MVDR Algorithm. *Appl. Sci.* **2023**, *13*, 8337. https://doi.org/10.3390/app13148337

Academic Editor: Amalia Miliou

Received: 20 May 2023
Revised: 7 June 2023
Accepted: 8 June 2023
Published: 19 July 2023

Copyright: © 2023 by the authors. Licensee MDPI, Basel, Switzerland. This article is an open access article distributed under the terms and conditions of the Creative Commons Attribution (CC BY) license (https://creativecommons.org/licenses/by/4.0/).

1. Introduction

Satellite communication is widely used in civilian and military communication due to its advantages of wide coverage, large communication capacity, and no geographical restrictions [1,2]. With the rapid development of military technology, information warfare has become an important form of modern warfare, and jamming and anti-jamming have naturally become the key combat methods that countries' armies are competing to research. Satellite communication faces three different jamming risks: uplink jamming, downlink jamming, and inter-satellite link jamming [3]. Downlink jamming requires low power, controllable range of influence, and is not easily detected by the other party, making it suitable for local wars under information conditions. Portable small satellite communication ground station antennas have a small diameter, simple structure, and a large number, but they have few anti-jamming measures and weak capabilities. When their downlink is interfered with, the communication quality seriously deteriorates, and even the received signal-to-noise ratio is lower than the threshold, causing communication interruption, so it is urgent to improve their anti-jamming capabilities.

Anti-jamming technologies for earth stations mainly include spread spectrum technology, coding and modulation technology, and adaptive nulling antenna technology [4]. Direct sequence spread spectrum [5] spreads the baseband signal over a wide spectrum, effectively resisting narrowband signal jamming. However, the spreading code consisting of pseudo-random sequences has a rate much greater than the information rate, with one information bit width equal to multiple periods of the pseudo-random sequence, resulting in lower spectrum utilization. Frequency hopping technology [6] rapidly and discretely

changes the carrier frequency according to a preset rule, making it difficult for jamming to target the signal frequency, thus ensuring reliable transmission of information. However, its anti-tracking jamming effect is limited. Coding and modulation technology encodes the baseband signal according to certain rules and converts it into a modulated signal suitable for transmission in the channel, effectively improving the reliability and efficiency of the communication system. It is widely used in modern communication. Adaptive nulling antenna technology aligns the nulls with the direction of the jamming signal by weighting the antenna array elements, achieving effective suppression of jamming [7]. Time-domain filtering anti-jamming technology is simple to implement, with low costs and anti-narrowband jamming ability of 10–35 dB, but not ideal for filtering wideband jamming signals. Antenna anti-jamming technology is mature, flexible, and has a high degree of freedom, so multiple satellite earth station antennas can be arrayed and adaptive beamforming technology can be used to improve the anti-jamming ability of the satellite earth station array. The MVDR [8] algorithm is a typical adaptive beamforming technology that minimizes the output power of jamming and noise while keeping the array output power constant, thus effectively suppressing jamming. The MVDR algorithm is a classic spatial filtering algorithm that can improve the receiver's anti-jamming performance by about 40–50 dB. However, the traditional MVDR algorithm is sensitive to errors in the source direction and element, and its beamformer performance severely degrades when errors exist. Based on this, Carlson B D proposed the diagonal loading-based MVDR algorithm [9], which improves the robustness of the MVDR algorithm.

Currently, the MVDR algorithm is widely used in radar, communication, sonar, signal processing, and other fields [10]. Reference [11] uses the MVDR algorithm in beam-domain preprocessing to reduce the impact of strong jamming outside the beam domain on high-resolution wave direction estimation algorithms. Reference [12] replaces the traditional one-dimensional uniform linear frequency control array structure with a frequency control array multi-input multi-output structure and combines the MVDR algorithm to suppress external jamming outside the platform. Reference [13] uses a joint graph Fourier transform to map multi-channel noisy speech signals to the graph frequency domain. Based on the characteristics of the graph frequency domain, the MVDR algorithm is designed to enhance multi-channel noisy speech signals and improve speech quality and intelligibility. Based on the above analysis, the MVDR algorithm can effectively suppress external jamming in various scenarios, but the scenarios mainly focus on array forms where the distance between elements meets half-wavelength and do not consider the impact of signal incidence angle on signal gain.

This article addresses the problem of a decrease in communication quality or even communication interruption caused by jamming to the downlink of satellite communication earth station. Firstly, the expression of the gain of a reflector antenna is deduced based on the calculation method of the maximum gain of an antenna, the pointing error of the antenna, and the maximum gain constraint of the sidelobe, and a mathematical model for the receiving signal of the reflector antenna array is established. Since the antenna elements are reflector antennas for the earth station, their gain varies with the direction of the incident signal. Therefore, a MVDR beamforming algorithm based on reflector antennas is proposed and applied to the satellite communication earth station array. Then, by using computer simulation with variables of the number of snapshots and satellite signal power flux density, the effectiveness of the proposed algorithm relative to conventional beamforming and the algorithm based on the sampling matrix inversion is verified. The output SINR of the array with different jamming incident angles is simulated by setting actual parameters of the satellite communication system, and the reason for the poor jamming resistance performance at some angles is theoretically derived.

2. Satellite Communication Earth Station Array Model

Reflector antennas have the advantages of simple structure and good directionality. Portable small satellite communication earth stations usually use this type of antenna, with a gain of [14]

$$[G(0)] = 10\lg\left(\frac{4\pi A\eta}{\lambda^2}\right) = 10\lg\left(\left(\frac{\pi D}{\lambda}\right)^2\eta\right) \tag{1}$$

In the formula, A is the antenna area, D is the antenna diameter, λ is the signal wavelength, and η is the antenna efficiency. Variables in this article with square brackets represent their dB values.

The half-power beamwidth of the antenna can be expressed as

$$\theta_{1/2} = 70^\circ\frac{\lambda}{D} \tag{2}$$

When the error of the antenna main beam deviation from the satellite direction (antenna pointing error) is less than half the power beamwidth, the antenna gain can be estimated using the following formula [15]

$$[G(\theta)] = [G(0)] - 12\left(\frac{\theta}{\theta_{1/2}}\right)^2 \tag{3}$$

In the formula, θ is the antenna pointing error.

When the ratio of the diameter of the receiving antenna to the wavelength is less than 50, the gain of the antenna sidelobes is not greater than the following formula [16,17]

$$[G(\theta)] = \begin{cases} 32 - 25\lg\theta & 100^\circ\frac{\lambda}{D} \le \theta \le 48^\circ \\ -10 & \theta > 48^\circ \end{cases} \tag{4}$$

In this article, Equation (4) is used to represent the antenna gain for the corresponding angle. The gains of point and point are connected by a straight line to represent the antenna gain between two angles (the method of representing negative angle gains is similar). Therefore, the gain of the satellite communication earth station reflector antenna can be expressed as

$$[G(\theta)] = \begin{cases} 10\lg\left(\left(\frac{\pi D}{\lambda}\right)^2\eta\right) - 12\left(\frac{\theta}{\theta_{1/2}}\right)^2 & |\theta| \le 35^\circ\frac{\lambda}{D} \\ \frac{\beta}{\gamma} + 10\lg\left(\left(\frac{\pi D}{\lambda}\right)^2\eta\right) - 3 & 35^\circ\frac{\lambda}{D} < |\theta| \le 100^\circ\frac{\lambda}{D} \\ 32 - 25\lg\theta & 100^\circ\frac{\lambda}{D} < |\theta| \le 48^\circ \\ -10 & |\theta| > 48^\circ \end{cases} \tag{5}$$

In the formula, β and γ can be expressed as

$$\beta = 35 - 10\lg\left((100)^{\frac{5}{2}}\pi^2\eta\left(\frac{\lambda}{D}\right)^{\frac{1}{2}}\right) \tag{6}$$

$$\gamma = 65\frac{\lambda}{D\cdot\left(\theta - \frac{1}{2}\theta_{1/2}\right)} \tag{7}$$

Consider N narrowband signals/jammings entering the uniform linear array composed of reflector antennas of the earth station (as shown in Figure 1) in the far field. Assuming that the angle between the earth station reflector antenna and the satellite is 0°, the jamming is in the plane composed of the array and the incoming wave from the satellite. The distance between the reflector antennas is d, and the first reflector antenna on

the left (point *O*) is the reference antenna. Then, the position of the lth reflector antenna is $((l-1)\,d,0)$.

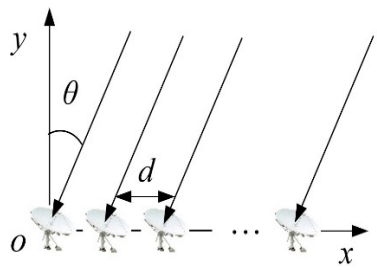

Figure 1. Linear array of reflector antennas.

Assuming that the signal incident angle is θ_0, the i-th jamming incident angle is θ_i, and the gain of the earth station reflector antenna for it satisfies Equation (5), let the gain of the lth reflector antenna for the signal be $[G_l(\theta_0)]$, and the gain for the i-th jamming be $[G_l(\theta_i)]$. The received data output of the M reflector antennas at time t is arranged into a column vector [18], which can be obtained as follows

$$\boldsymbol{x}(t) = \boldsymbol{A}\boldsymbol{s}(t) + \boldsymbol{n}(t) \tag{8}$$

In the formula, $\boldsymbol{x}(t) = [x_1(t)\ x_2(t)\ \cdots\ x_M(t)]^{\mathrm{T}}$ is the M × 1-dimensional snapshot data vector of the array, $\boldsymbol{n}(t) = [n_1(t)\ n_2(t)\ \cdots\ n_M(t)]^{\mathrm{T}}$ is the M × 1-dimensional noise data vector of the array, and $s(t) = [s_0(t)\ s_1(t)\ \cdots\ s_{N-1}(t)]^{\mathrm{T}}$ is the N × 1-dimensional vector of spatial signals and jammings, where $s_0(t)$ and $s_i(t)$ are the complex envelopes of the signal and the i-th jamming at time t, respectively, $(\bullet)^{\mathrm{T}}$ represents the transpose operation, and $\boldsymbol{A}$ is the array manifold matrix, which can be expressed as

$$\boldsymbol{A} = \begin{bmatrix} \hat{\boldsymbol{a}}(\theta_0) & \hat{\boldsymbol{a}}(\theta_1) & \cdots & \hat{\boldsymbol{a}}(\theta_{N-1}) \end{bmatrix} \tag{9}$$

In the formula, $\hat{\boldsymbol{a}}(\theta_i)$ is the directional vector of the signal/jamming, which can be expressed as

$$\hat{\boldsymbol{a}}(\theta_i) = \boldsymbol{Q}(\theta_i)\boldsymbol{a}(\theta_i) = \begin{bmatrix} Q_1(\theta_i) \\ Q_2(\theta_i)\mathrm{e}^{\frac{-\mathrm{j}2\pi d\sin\theta_i}{\lambda}} \\ \vdots \\ Q_M(\theta_i)\mathrm{e}^{\frac{-\mathrm{j}2\pi(M-1)d\sin\theta_i}{\lambda}} \end{bmatrix} \tag{10}$$

where $Q_l(\theta_i)$ is the influence of the antenna on the amplitude of the signal/jamming, and $G_l(\theta_i)$ is the gain of the antenna on the power of the signal/jamming, that is $Q_l(\theta_i) = 10^{[G_l(\theta_i)]/20}$.

It can be derived from Equation (10)

$$\boldsymbol{Q}(\theta_i) = \mathrm{diag}[Q_1(\theta_i), Q_2(\theta_i), \cdots, Q_M(\theta_i)] \tag{11}$$

$$\boldsymbol{a}(\theta_i) = \left[1, \mathrm{e}^{\frac{-\mathrm{j}2\pi d\sin\theta_i}{\lambda}}, \cdots, \mathrm{e}^{\frac{-\mathrm{j}2\pi(M-1)d\sin\theta_i}{\lambda}}\right]^{\mathrm{T}} \tag{12}$$

Equation (12) is the directional vector of the array receiving signal/jamming composed of isotropic elements.

3. Satellite Communication Earth Station Array MVDR Algorithm

The MVDR algorithm is based on the minimum mean square error criterion, which ensures that the output power of the beamformer is minimized while the gain in the constrained target direction remains constant. This means that the jamming and noise

power are minimized, achieving suppression of jamming and noise. In this article, the constrained target is the satellite signal received by the earth station, and the goal is to minimize the total power of jamming and noise signals received by the earth station, thereby maximizing the array output SINR. Assuming that the satellite signal is incident from direction θ_0 and N − 1 jammings are incident from directions θ_i (i = 1, 2, . . . , N − 1), the output of the linear array at time t is [19]

$$\boldsymbol{x}(t) = \boldsymbol{x}_{\mathrm{S}}(t) + \boldsymbol{x}_{\mathrm{I}}(t) + \boldsymbol{n}(t) \tag{13}$$

where $\boldsymbol{x}_{\mathrm{S}}(t) = \hat{\boldsymbol{a}}(\theta_0)\boldsymbol{x}_0(t)$, $\boldsymbol{x}_{\mathrm{I}}(t) = \sum_{i=1}^{N} \hat{\boldsymbol{a}}(\theta_i)\boldsymbol{x}_i(t)$, and $n(t)$ represent the signal, jamming, and noise, respectively, and $\hat{\boldsymbol{a}}(\theta_0)$ and $\hat{\boldsymbol{a}}(\theta_i)$ are the steering vectors of the signal and jamming, respectively.

The covariance matrix of jamming and noise can be derived as [20]

$$\begin{aligned} \boldsymbol{R}_{\mathrm{i+n}} &= E\left\{(\boldsymbol{x}_{\mathrm{I}}(t) + \boldsymbol{n}(t))(\boldsymbol{x}_{\mathrm{I}}(t) + \boldsymbol{n}(t))^{\mathrm{H}}\right\} \\ &= \sum_{i=1}^{N-1} \sigma_i^2 \boldsymbol{Q}(\theta_i)\boldsymbol{\alpha}(\theta_i)\boldsymbol{\alpha}^{\mathrm{H}}(\theta_i)\boldsymbol{Q}^{\mathrm{H}}(\theta_i) + \sigma_{\mathrm{n}}^2 \boldsymbol{I} \end{aligned} \tag{14}$$

where σ_i^2 represents the power of the i-th jamming, σ_n^2 represents the power of the noise, I represents the M × M dimensional identity matrix, E{•} represents the expectation operation, and $(\bullet)^{\mathrm{H}}$ represents the conjugate transpose operation.

Assuming that the weight of the l-th element is w_l, the weight vector of the M elements can be arranged into a column vector [21]

$$\boldsymbol{w} = \begin{bmatrix} w_1 & w_2 & \cdots & w_M \end{bmatrix}^{\mathrm{T}} \tag{15}$$

The output of the array is the product of its weight vector and the received data

$$y(t) = \boldsymbol{w}^{\mathrm{H}}\boldsymbol{x}(t) = \sum_{l=1}^{M} w_l^* \boldsymbol{x}_l(t) \tag{16}$$

where $(\bullet)^*$ represents the conjugate operation.

From the above equations, the signal to interference plus noise ratio (SINR) of the array output can be derived as

$$\Psi = \frac{\sigma_s^2 \left|\boldsymbol{w}^{\mathrm{H}}\boldsymbol{Q}(\theta_0)\boldsymbol{a}(\theta_0)\right|^2}{\boldsymbol{w}^{\mathrm{H}}\boldsymbol{R}_{\mathrm{i+n}}\boldsymbol{w}} \tag{17}$$

where $\boldsymbol{Q}(\theta_0)\boldsymbol{a}(\theta_0)$ is the steering vector of the signal, and $\sigma_s{}^2$ is the power of the signal.

To minimize the jamming and noise power of the array output under the condition that the output of the expected direction signal is constant, the cost function can be constrained as [22]

$$\begin{cases} \min\limits_{w} \boldsymbol{w}^{\mathrm{H}}\boldsymbol{R}\boldsymbol{w} \\ \text{s.t.} \quad \boldsymbol{w}^{\mathrm{H}}\boldsymbol{Q}(\theta_0)\boldsymbol{a}(\theta_0) = 1 \end{cases} \tag{18}$$

where $\boldsymbol{R}$ represents the covariance matrix of the array's received data.

From Equation (18), it can be seen that to calculate the optimal weight vector of the MVDR algorithm, the covariance matrix of the array's received data must be obtained, but in practical situations, the array's sampling data is obtained instead. Therefore, under a certain sampling rate, the array's sampling covariance matrix can be used to replace the array's received data covariance matrix.

$$\begin{aligned} \boldsymbol{R}_{xx} &= \frac{1}{K}\sum_{i=1}^{K} \boldsymbol{x}\boldsymbol{x}^{\mathrm{H}} \\ &= \sum_{i=0}^{N-1} \sigma_i^2 \boldsymbol{Q}(\theta_i)\boldsymbol{a}(\theta_i)\boldsymbol{a}^{\mathrm{H}}(\theta_i)\boldsymbol{Q}^{\mathrm{H}}(\theta_i) + \sigma_n^2 \boldsymbol{I} \end{aligned} \tag{19}$$

where K represents the number of sampling data snapshots.

Thus, Equation (18) can be transformed into

$$\begin{cases} \min\limits_{w} \boldsymbol{w}^{\mathrm{H}}\boldsymbol{R}_{xx}\boldsymbol{w} \\ \text{s.t.} \quad \boldsymbol{w}^{\mathrm{H}}\boldsymbol{Q}(\theta_0)\boldsymbol{a}(\theta_0) = 1 \end{cases} \tag{20}$$

Using the Lagrange multiplier method, Equation (20) can be transformed into an unconstrained problem. Introducing the Lagrange factor μ and constructing the function

$$\mathrm{L}(w) = \frac{1}{2}\boldsymbol{w}^{\mathrm{H}}\boldsymbol{R}_{xx}\boldsymbol{w} - \mu\left[\boldsymbol{w}^{\mathrm{H}}\boldsymbol{Q}(\theta_0)\boldsymbol{a}(\theta_0) - 1\right] \tag{21}$$

Differentiating Equation (21) with respect to $\boldsymbol{w}$ and setting it to zero, the function with respect to the weight vector $\boldsymbol{w}$ can be obtained

$$\frac{\partial L}{\partial w} = \boldsymbol{R}_{xx}\boldsymbol{w} - \mu\boldsymbol{Q}(\theta_0)\boldsymbol{a}(\theta_0) = 0 \tag{22}$$

The optimal weight vector can be solved as

$$\boldsymbol{w} = \mu\boldsymbol{R}_{xx}^{-1}\boldsymbol{Q}(\theta_0)\boldsymbol{a}(\theta_0) \tag{23}$$

Then, using the constraint condition $\boldsymbol{w}^{\mathrm{H}}\boldsymbol{Q}(\theta_0)\boldsymbol{a}(\theta_0) = 1$, the Lagrange factor can be obtained as

$$\mu = \frac{1}{\boldsymbol{a}^{\mathrm{H}}(\theta_0)\boldsymbol{Q}^{\mathrm{H}}(\theta_0)\boldsymbol{R}_{xx}^{-1}\boldsymbol{Q}(\theta_0)\boldsymbol{a}(\theta_0)} \tag{24}$$

Substituting Equation (24) into Equation (23), the optimal weight vector can be obtained as

$$\boldsymbol{w} = \frac{\boldsymbol{R}_{xx}^{-1}\boldsymbol{Q}(\theta_0)\boldsymbol{a}(\theta_0)}{\boldsymbol{a}^{\mathrm{H}}(\theta_0)\boldsymbol{Q}^{\mathrm{H}}(\theta_0)\boldsymbol{R}_{xx}^{-1}\boldsymbol{Q}(\theta_0)\boldsymbol{a}(\theta_0)} \tag{25}$$

In practical communication environments, the performance of the traditional MVDR algorithm can sharply decrease due to factors such as external environment, antenna array, and estimation error of the sampling covariance matrix [23]. To address this, the diagonal loading MVDR algorithm can be used to improve the algorithm's robustness [24].

Let $\boldsymbol{R}_x = \boldsymbol{R}_{xx} + \delta\boldsymbol{I}$, the optimal weight vector of the diagonal loading MVDR algorithm can be represented as

$$\boldsymbol{w} = \frac{(\boldsymbol{R}_{xx} + \delta\boldsymbol{I})^{-1}\boldsymbol{Q}(\theta_0)\boldsymbol{a}(\theta_0)}{\boldsymbol{a}^{\mathrm{H}}(\theta_0)\boldsymbol{Q}^{\mathrm{H}}(\theta_0)(\boldsymbol{R}_{xx} + \delta\boldsymbol{I})^{-1}\boldsymbol{Q}(\theta_0)\boldsymbol{a}(\theta_0)} \tag{26}$$

The recommended range of the loading factor δ in the above equation is $\delta_S \leq \delta \leq \delta_L$, and the maximum loading level δ_L depends on the specific application, while the minimum loading level δ_S is generally not less than the noise power.

Due to the inclusion of matrix inversion algorithms in this article, its algorithmic complexity is at most cubic. Assuming the number of peak values in the Capon power spectrum is G, the complexity of the algorithm proposed in this article is $O(GSM^2 + GM^3 + N{\cdot}CM^2)$.

4. Simulation Analysis

Different from the MVDR algorithm that assumes the array elements are isotropic point sources, in this paper, the array elements are satellite communication earth station reflector antennas with gain following Equation (5), and therefore, the directional vector of the array receiving signal follows Equation (10).

Assuming that the array in this paper is a uniform linear array composed of identical satellite communication earth station reflector antennas, the array deployment method is

the same as that required in Section 2. Considering the actual jamming scenario of satellite communication downlink, the jamming direction may vary, so the power flux density (PFD) at the earth station antenna is used to represent the size of the signal and jamming. The power after passing through the antenna can be calculated using the following equation

$$[P] = [F] + [G(\theta)] + 10\lg\left(\frac{\lambda^2}{4\pi}\right) \tag{27}$$

Here, $[F]$ represents power flux density. The power flux density of the signal is set according to the actual size, with a reflector antenna diameter of D = 0.5 m, antenna efficiency of η = 0.7, signal frequency of f = 12.5 GHz, and the expected signal wave direction of $\theta_0 = 0°$. The incident angle range is $-90° \leq \theta \leq 90°$. Since the diagonal loading method used in this paper is an optimization problem under the worst performance, the size of the diagonal loading has little effect on the performance of the algorithm within a certain range [25]. Therefore, in this experiment, the diagonal loading amount uses noise power and Matlab 2016.

4.1. Two Beamforming Methods and Single Antenna Gain

In this section, the conventional beamforming (CBF) and MVDR algorithms are used with four reflector antennas, with a spacing of $d = c/(2 \times f) \times 42 = 0.504$ m, a snapshot of 512, an jamming direction of $\theta_1 = 10°$, a signal power flux density of -110 dBW/m^2, an jamming power flux density of -80 dBW/m^2, and a noise power of -133.38 dBW.

Without jamming, the array gain using CBF and MVDR algorithms is the same. The difference between the two algorithms when jamming is present lies in the assignment of weight vectors. However, since the signal direction in this paper is 0°, the array gain in the signal direction is the same for both algorithms. To facilitate comparison, the maximum gain in the 0° direction of the MVDR beamforming diagram is set to be the same as that of the CBF beamforming diagram. From Figures 2 and 3, it can be seen that after four satellite communication earth station reflector antennas are arranged into a uniform linear array, the maximum gain using CBF and MVDR algorithms is about 46.8 dB, which is 12 dB higher than the maximum gain of a single satellite earth station reflector antenna in Figure 4 (34.8 dB). The array gain in the 10° direction using CBF algorithm is about 7.6 dB, while using the MVDR algorithm with diagonal loading, a null is formed in the direction of the jamming (the jamming direction corresponding to the normalized gain in the signal direction), and the gain is about -15.4 dB. The gain of a single earth station in the 10° direction is 7 dB. Therefore, it can be concluded that when the jamming direction is 10°, using CBF and MVDR algorithms with diagonal loading can improve the signal gain and suppress the jamming, and the MVDR algorithm has a better jamming suppression effect.

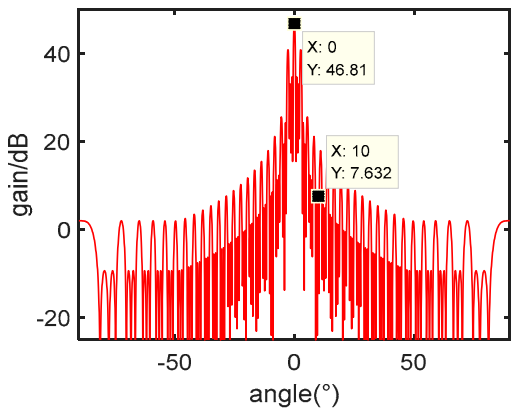

Figure 2. CBF pattern of antenna array.

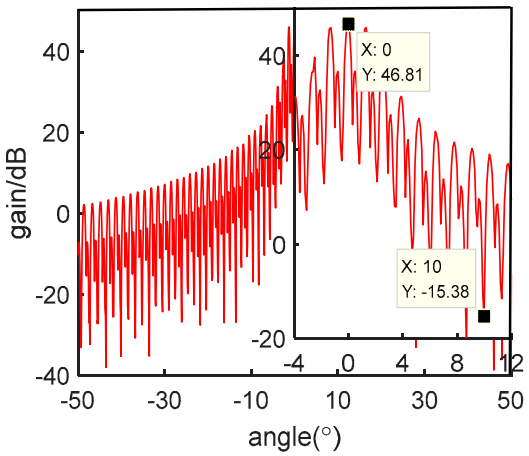

Figure 3. MVDR pattern of antenna array.

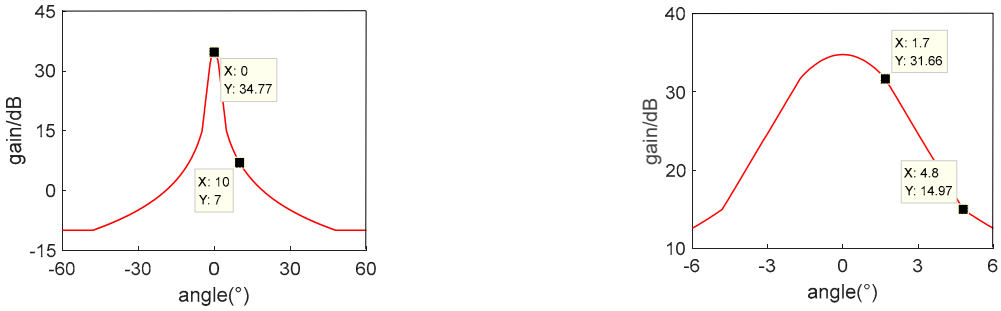

(**a**) −60°~60° (**b**) Local enlarged pattern

Figure 4. Proposed antenna gain of earth station (D = 0.5 m).

4.2. Jamming Suppression Effect under Different Parameters

To verify the universality of the proposed algorithms for jamming suppression in satellite communication earth station antenna arrays, three simulation experiments are conducted with four reflector antennas, a spacing of d = c/(2 × f) × 42 = 0.504 m, a noise power of −131.28 dBW, an jamming power flux density of −80 dBW/m^2, and varying jamming angles, snapshot sizes, and signal power flux densities. The results are the average of 200 Monte Carlo simulations.

Experiment 1: Different Snapshots. To investigate the effect of snapshots on the jamming suppression performance of the MVDR algorithm, 10 snapshots ranging from 100 to 1000 are set with an interval of 100. In addition, the jamming direction is $\theta_1 = 10°$, and the signal power flux density at the reflector antenna is −110 dBW/m^2.

From Figure 5, it can be seen that as the snapshots increases, the depth of null in the jamming direction using the MVDR algorithm with diagonal loading also increases, but the increase rate gradually slows down. The output SINR of the array also increases gradually, but the increase rate slows down after reaching a certain snapshot. Therefore, to achieve ideal jamming suppression performance while keeping the computational complexity reasonable, an appropriate snapshot needs to be selected. In addition, it can be seen that the output SINR of the algorithm proposed in this article is higher than that of the algorithm based on the sampling matrix inversion method at the same snapshots.

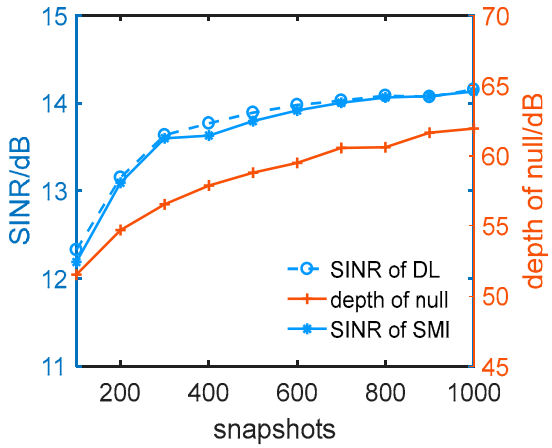

Figure 5. Output SINR and depth of null versus the number of snapshots.

Experiment 2: Different Signal PFD. To investigate the effect of signal power flux density at the reflector antenna on the jamming suppression performance of the MVDR algorithm, seven sets of data with signal PFD ranging from -110 dBW/m^2 to -80 dBW/m^2 in increments of 5 dB are set. In addition, the jamming direction is $\theta_1 = 10^\circ$, and the number of snapshots is 512.

From Figures 6 and 7, it can be seen that as the signal PFD at the reflector antenna increases, the depth of null in the jamming direction gradually decreases. Within the range of experimental data, the output SINR of the array using the MVDR algorithm with diagonal loading is the highest, followed by the array using the CBF algorithm, and the single antenna has the lowest output SINR. The output SINR of the MVDR algorithm with diagonal loading gradually slows down as the input SNR increases, while the output SINR of the CBF algorithm and the single antenna increases linearly with the input SNR. This indicates that the jamming suppression effect of the MVDR algorithm in satellite communication earth station antenna arrays deteriorates as the input SNR increases. This is because the algorithm uses the sample covariance matrix to replace the jamming plus noise covariance matrix, and high SNR leads to relatively small jamming plus noise power, resulting in a deterioration of jamming suppression effect.

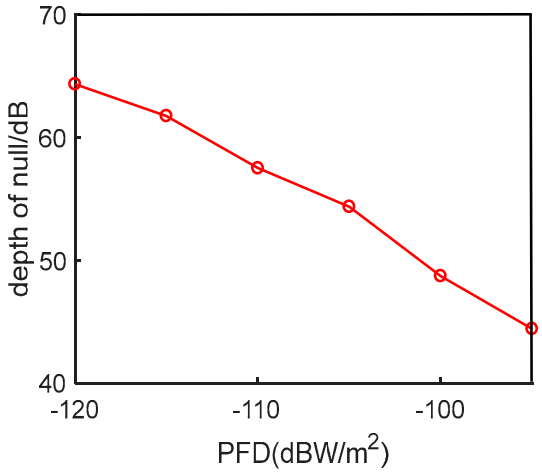

Figure 6. Depth of null versus PFD.

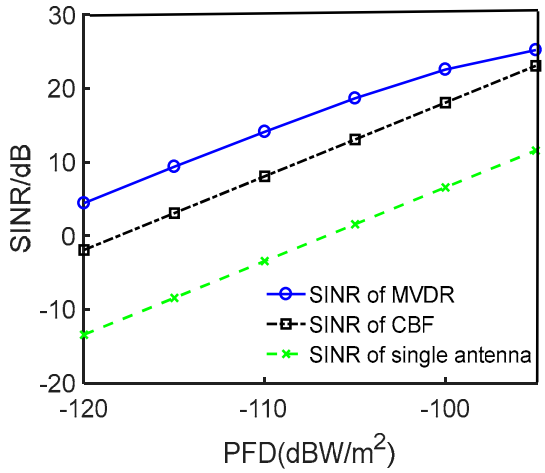

Figure 7. Output SINR versus PFD.

4.3. Jamming Suppression Performance in Actual Satellite Communication

When there is jamming in the downlink(as shown in Figure 8), assuming that the jamming frequency is the same as the satellite downlink signal frequency, the signal/jamming power at the input of the satellite communication earth station receiver is without the polarization mismatch loss of the receiving and transmitting antennas, the receiving antenna pointing loss and the transmitting antenna pointing loss [26] can be expressed as

$$[P] = [E] + [G(\theta)] - [L_{FS}] - [L_{RF}] - [L_A] \tag{28}$$

where $[E]$ is the effective isotropic radiated power (EIRP) of the satellite/jamming source, $[G(\theta)]$ is the gain of the antenna for the satellite signal/jamming, $[L_{RF}]$ is the loss of the feeder, $[L_A]$ is the atmospheric absorption loss, and $[L_{FS}]$ is the free space propagation loss of the satellite signal/jamming, which can be expressed as

$$[L_{FS}] = 92.44 + 20\lg z(\text{km}) + 20\lg f(\text{GHz}) \tag{29}$$

where z is the propagation distance of the signal/jamming, and f is the frequency of the signal/jamming.

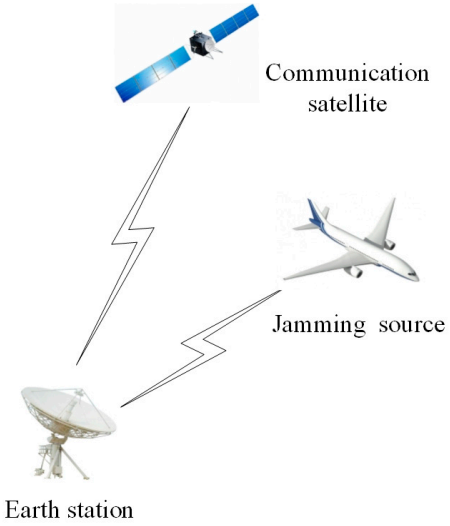

Figure 8. A satellite communication system with the downlink jamming.

The distance between the satellite and the earth station can be calculated as

$$z_s = 42164 \times \sqrt{1.023 - 0.303 \cos e \cos \Delta g} \quad (\text{km}) \tag{30}$$

where e is the latitude of the earth station, and Δg is the difference between the longitude of the earth station and the longitude of the satellite sub-point.

The noise power is

$$[N] = 10\text{lg}(kTB) \tag{31}$$

where $k = 1.38 \times 10 - 23$ J/k is the Boltzmann constant, T is the equivalent noise temperature of the earth station receiving system, and B is the noise bandwidth.

The power flux density at a distance of z from the transmitting antenna can be expressed as

$$[F] = [E] - 20\text{lg}z(\text{m}) - 10.99 \tag{32}$$

After experimental simulation and literature review, SINR enhancement effects of 5 MVDR algorithms are shown in Table 1. In order to test the effectiveness of the proposed algorithm in the actual satellite communication system, the following experiments are carried out. Assuming that the satellite in this experiment is a geostationary orbit communication satellite, and the specific parameters of the satellite, earth station, and jamming source are shown in Table 2. The distance between the satellite and the earth station is z_s = 37,045 km. The satellite signal flux density at the earth station antenna is -110.36 dBW/m^2, and the satellite signal power after passing through the earth station antenna is -119.98 dBW. The noise power is -131.28 dBW.

Table 1. Comparison of different methods for anti-jamming effect.

Method	SINR Improvement
CBF algorithm	29 dB
SMI algorithm	34.6 dB
Jamming signal separation method	28 dB
Despread–respread method	30.1 dB
DL algorithm	36 dB

Table 2. The parameters of satellite communication system.

Parameter	Value
Downlink signal frequency	12.5 GHz
Satellite fixed-point longitude	110.5° E
Earth station antenna diameter	0.5 m
Earth station longitude	108.5° E
Earth station latitude	34° N
EIRP of the satellite	52 dBW
Atmospheric absorption loss	0.5 dB
Feeder loss	0.5 dB
Altitude of the jamming source	5 km
Equivalent noise temperature of the earth station	150 K
Noise bandwidth	36 MHz
SNR threshold of the earth station	7 dB

In experiment 3, assuming that the incident angle of the jamming source is 10°, the EIRP of the jamming source is set from -20 dBW to 10 dBW.

From Figure 9, it can be seen that when the EIRP of the jamming source is -7.18 dBW and 5.37 dBW, the output SINR of the single antenna and the array based on the CBF algorithm is about 7 dB, reaching the SNR threshold of the earth station. Within the range of experimental data, the output SINR of the array based on the MVDR algorithm with diagonal loading is about 12 dB, exceeding the SNR threshold of the earth station. Therefore, when the EIRP of the jamming source is less than -7.18 dBW, the single antenna,

the array based on the CBF algorithm, and the array based on the MVDR algorithm with diagonal loading can all communicate normally. When −7.18 dBW < EIRP of the jamming source < 5.37 dBW, the single antenna cannot communicate normally, and the array based on the CBF algorithm and the array based on the MVDR algorithm with diagonal loading can communicate normally. When the EIRP of the jamming source is greater than 5.37 dBW, only the array based on the MVDR algorithm with diagonal loading can communicate normally.

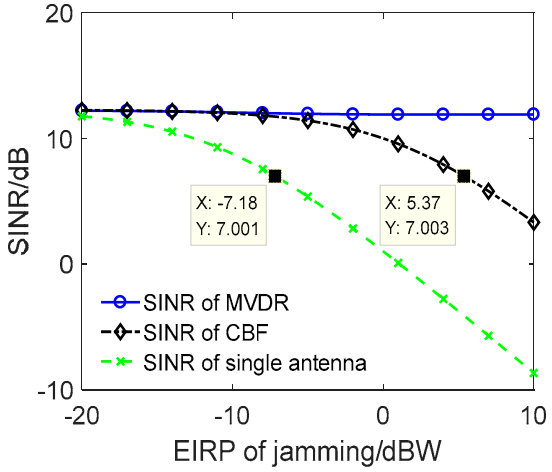

Figure 9. Output SINR versus EIRP of jamming.

In experiment 4, assuming that the EIRP of the jamming source is −5 dBW, the incident angle of the jamming source is set from 5° to 80° with an interval of 0.1°.

From Figure 10, it can be seen that when the incident angle of the jamming source is 28.1° (the distance between the jamming source and the earth station antenna is 5.67 km), the output SINR of the single antenna is about 7.01 dB, and the output SINR of the earth station array based on the CBF algorithm and the array based on the MVDR algorithm with diagonal loading is greater than 7.01 dB, exceeding the SNR threshold of the earth station. When the incident angle of the jamming source is less than 28.1°, the output SINR of the earth station array based on the MVDR algorithm with diagonal loading is greater than 7 dB at most angles. Therefore, when the incident angle of the jamming source is $\leq -28.1°$ or $\geq 28.1°$, the single antenna, the array based on the CBF algorithm, and the array based on the MVDR algorithm with diagonal loading can all communicate normally. When $-28.1° <$ incident angle of the jamming source $< 28.1°$, the single antenna cannot communicate normally, the earth station array based on the CBF algorithm can only communicate at fewer angles than the array based on the MVDR algorithm with diagonal loading. Based on statistics within the range of angles in this experiment, assuming that the incident angle of the jamming source is uniformly distributed, the probability that the earth station array based on the MVDR algorithm with diagonal loading can communicate normally is over 95%.

In addition, it was found by calculation that there are angles in Figure 10 where the jamming suppression performance of the CBF algorithm and the MVDR algorithm with diagonal loading is poor. This is because the signal angle in this experiment is 0°, resulting in $a(\theta_0) = [1,1,1,1]^T$, and the above angle $a(\theta_i)$ is very close to $a(\theta_0)$. Moreover, the antenna elements in this experiment are four completely identical planar antennas, so $Q(\theta_i)a(\theta_i) = Q(\theta_i)a(\theta_i)$, and the directional vectors of the satellite signal and the jamming signal can be, respectively, represented as $Q(\theta_0)a(\theta_0)$ and $Q(\theta_i)a(\theta_i)$. Then, $w^H Q(\theta_0)a(\theta_0)/(w^H Q(\theta_i)a(\theta_i)) \approx Q(\theta_0)/Q(\theta_i)$, so the output SINR of the array is approximately equal to that of the single antenna. In this experiment, the amplified jamming power after the antenna is much greater than the noise power, resulting in a small contribution of the noise power to the output SINR of the MVDR algorithm and the single antenna.

Therefore, the output SINR of the array based on the MVDR algorithm with diagonal loading is approximately equal to that of the single antenna at the above angles, resulting in poor jamming suppression performance of the MVDR algorithm with diagonal loading. The CBF algorithm can be understood as a special case of the MVDR algorithm with all weight values equal.

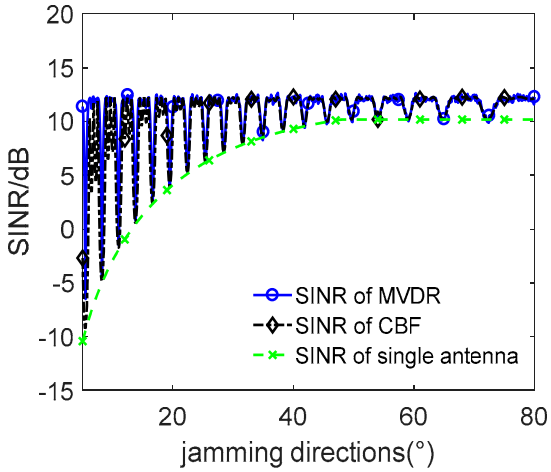

Figure 10. Output SINR versus jamming directions.

5. Conclusions

In response to the problem of communication quality degradation or even interruption caused by downlink jamming in satellite communication earth stations, this paper constructs a reflector antenna array model, derives the corresponding MVDR beamforming algorithm, and applies the algorithm in the reflector antenna array of satellite communication earth stations. Finally, the algorithm is simulated and analyzed using Matlab 2016. The simulation results show that using multiple satellite communication earth stations to form an array, and using the MVDR beamforming algorithm to assign certain weights to signals from different directions, can improve the directional gain of satellite signals, effectively suppress jamming, and enhance the SINR of the array output. Furthermore, the jamming suppression effect gradually improves with an increase in snapshots. However, the proposed algorithm has poor anti-jamming performance at some angles, and further optimization of the algorithm and array layout is needed to improve the range of jamming suppression for the array.

Author Contributions: Software, J.L.; Formal analysis, Y.X.; Investigation, W.Z.; Writing—original draft, Y.X. All authors have read and agreed to the published version of the manuscript.

Funding: This paper was supported by the National Natural Science Foundation of China (No. 62271500), Natural Science Research Fund Program of Shaanxi (No. 2020JM-344), and Graduate Innovation Practice Fund of Air Force Engineering University (No. CXJ2022024).

Data Availability Statement: Data is unavailable due to privacy.

Acknowledgments: We appreciate Wei Li's professional guidance during the writing and revision of the paper. The authors thank the anonymous reviewers for offering extraordinary advice.

Conflicts of Interest: The authors declare no conflict of interest.

References

1. Li, Y.; Li, K.X.; Wang, J.H.; Gao, X.; Xia, X.-G.; Ottersten, B. Massive MIMO transmission for LEO satellite communications. *IEEE J. Sel. Areas Commun.* **2020**, *38*, 1851–1865.
2. Zhao, J.; Gao, F.; Wu, Q.; Jin, S.; Wu, Y.; Jia, W. Beam Tracking for UAV Mounted SatCom on-the-Move with Massive Antenna Array. *IEEE J. Sel. Areas Commun.* **2018**, *36*, 363–375. [CrossRef]

3. Wang, Q.; Wang, L.T.; Wang, Y.; Yuan, L.; Xiong, Y.; Li, W. Analysis of jamming positioning technology in satellite communication. In Proceedings of the 2021 4th International Conference on Advanced Electronic Materials, Computers and Software Engineering, Changsha, China, 26–28 March 2021; IEEE Press: New York, NY, USA, 2021.
4. Zhao, Y.; Wang, S.L.; Wang, H.; Zhao, L.J. Evaluation of anti-jamming effectiveness of satellite communication based on cloud model. *Telecommun. Eng.* **2022**, *62*, 311–316.
5. Choi, H.; Moon, H. Blind Estimation of Spreading Sequence and Data Bits in Direct-Sequence Spread Spectrum Communication Systems. *IEEE Access* **2020**, *99*, 148066–148074. [CrossRef]
6. Man, J.; Li, W.; Ma, W. On the technology of frequency hopping communication network-station selection. In Proceedings of the 2021 International Conference on Electronics, Circuits and Information Engineering, Zhengzhou, China, 22–24 January 2021; IEEE Press: New York, NY, USA, 2021.
7. Yang, L. Research on Anti-Jamming Technology in Satellite Mobile Communication System. Ph.D. Thesis, Southeast University, Nanjing, China, 2021.
8. Capon, J. High-resolution frequency-wavenumber spectrum analysis. *Proc. IEEE* **1969**, *57*, 1408–1418. [CrossRef]
9. Carlson, B.D. Covariance matrix estimation errors and diagonal loading in adaptive arrays. *IEEE Trans. Aerosp. Electron. Syst.* **1988**, *24*, 397–401. [CrossRef]
10. Arnab, S.; Jared, S.; Aboulnasr, H. MVDR beamformer design by imposing unit circle roots constraints for uniform linear arrays. *IEEE Trans. Signal Process.* **2021**, *69*, 6116–6130.
11. You, H.; Huang, J.G.; Xu, G.M. Beamspace pre-processing on array data based on MVDR. *Syst. Eng. Electron.* **2008**, *30*, 64–67.
12. Chen, Y.; Tian, B.; Wang, C.Y.; Gong, J.; Tan, M.; Zhao, Y.J. FDA platform external jamming suppression based on MVDR beamforming. *Syst. Eng. Electron.* **2023**, *45*, 32–40. Available online: https://kns.cnki.net/kcms/detail/11.2422.TN.20220402.1443.010.html (accessed on 30 October 2022).
13. Yang, Y.; Guo, H.Y.; Wang, T.T.; Zhang, P.C.; Yang, Z. Multichannel speech MVDR enhancement algorithm based on joint spatial-temporal graph topology. *J. Signal Process.* **2023**, *39*, 540–549. Available online: http://kns.cnki.net/kcms/detail/11.2406.TN.20221008.1745.016.html (accessed on 15 November 2022).
14. Warnick, K.F.; Jeffs, B.D. Gain and aperture efficiency for a reflector antenna with an array feed. *IEEE Antennas Wirel. Propag. Lett.* **2006**, *5*, 499–502. [CrossRef]
15. Xu, Q.; Zhang, J.; Pan, H.Z. Analysis and compensation of the reflector antenna pointing error under wind disturbance. *Res. Astron. Astrophys.* **2021**, *6*, 387–396. [CrossRef]
16. *IESS-601*; Intelsat Earth Station Standards. Intelsat: Washington, DC, USA, 2005.
17. Guo, Y.; Kong, H.; Huang, Q.; Lin, M.; Zhu, W.; Amindavar, H. Performance analysis for the forward link of multiuser satellite communication systems. *Int. J. Satell. Commun. Netw.* **2021**, *39*, 560–569. [CrossRef]
18. Wang, Y.L.; Chen, H.; Peng, Y.N.; Wan, Q. Spatial Spectrum Estimation and Theoretical Algorithms. Master's Thesis, Tsinghua University, Beijing, China, 2004.
19. Sun, S.C.; Ye, Z.F. Robust adaptive beamforming based on a method for steering vector estimation and jamming covariance matrix reconstruction. *Signal Process.* **2021**, *182*, 107939. [CrossRef]
20. Yuan, X.L.; Lu, G. Robust adaptive beamforming via a novel subspace method for jamming covariance matrix reconstruction. *Signal Process.* **2016**, *130*, 233–242. [CrossRef]
21. Park, K.; Seo, J. Single-Antenna-Based GPS Antijamming Method Exploiting Polarization Diversity. *IEEE Trans. Aerosp. Electron. Syst.* **2021**, *27*, 919–934. [CrossRef]
22. Chen, P.; Yang, X.X.; Wang, Y.; Ma, Y. Adaptive beamforming with sensor position errors using covariance matrix construction based on subspace bases transition. *IEEE Signal Process. Lett.* **2019**, *26*, 19–23. [CrossRef]
23. Li, H.R.; Geng, J.; Xie, J.H. Robust adaptive beamforming based on covariance matrix reconstruction with RCB principle. *Digit. Signal Process.* **2022**, *127*, 103565. [CrossRef]
24. Yang, J.; Liu, R.Q.; Xi, X.Q. A adaptive beamforming design in low sample number conditions based on diagonal loading algorithm. In Proceedings of the 2016 IEEE International Conference on Signal and Image Processing, Beijing, China, 13–15 August 2016; IEEE Press: New York, NY, USA, 2016.
25. Shi, R.H.; Meng, Q.J.; Dong, J.; Guo, Y. A robust adaptive beamforming algorithm based on diagonal loading. *J. Hunan Univ.* **2012**, *39*, 57–61.
26. Min, S.Q. Satellite Communication System Engineering Design and Application. Master's Thesis, Publishing House of Electronics Industry, Beijing, China, 2004.

Disclaimer/Publisher's Note: The statements, opinions and data contained in all publications are solely those of the individual author(s) and contributor(s) and not of MDPI and/or the editor(s). MDPI and/or the editor(s) disclaim responsibility for any injury to people or property resulting from any ideas, methods, instructions or products referred to in the content.